RSC Advances

ARTICLE

Active porous valves for plug actuation and plug flow manipulation in open channel fluidics

Received 00th January 20xx,
Accepted 00th January 20xx

DOI: 10.1039/x0xx00000x

www.rsc.org/

N. Vourdas, K. Dalamagkidis, V.N. Stathopoulos

We present an alternative tool for plug actuation and valving on open-channel fluidics. Initially the fluidic walls are sticky and the plug is pinned (valve "off"). By applying pressure at the rear face of the wall (backpressure), the wall becomes slippery the plug is depinned and moves along the fluidic (valve "on"). We demonstrate the basic principles of the tool, and we provide experimental results on the minimum backpressure to leverage the actuation and the valve switching for fluidics of various cross-sections. Large cross-section fluidics may facilitate the control of a wide range of liquid volumes, at different operating parameters. For valves with small cross sections, the adequate backpressure is ultra-low (less than 10 mbar) corresponding to respectively ultra-low operation energy demands. In advance, for the small cross-section fluidics the backpressure is independent of the droplet volume and tilt angle, thus providing an attractive, versatile actuation and valving tool for low cost open channel fluidics.

Introduction

Incorporation of materials and devices with controllable and active wetting properties is now emerging as a key issue towards high-performance microfluidics and embedded systems.[1-6] Droplet actuation and valving on such systems call for tools that deliver wetting and mobility switching on-demand, with high throughput, low cost and large production amenability.[7-11] Desirable salient characteristics include also low energy demands,[12] high adaptability, ultra low actuation times and minimum interaction with the working liquid phase. Undesirable interactions may be chemical or through incorporation of particles or any other third-party substances, or thermal through temperature increase.

To this end a variety of passive[13-17] and active[18-23] tools, have been proposed for closed-channel fluidics[24], with electrowetting and related methodologies being the most successful alternatives.[25-27]

Less attention has been given to the development of actuation and valving tools for open channel fluidics,[28] namely fluidics where the channel is open on at least one side, digital microfluidics,[29, 30] and suspended microfluidics.[31] These devices call for respectively cheap, versatile, easy to fabricate and use peripherals, such as pumps and valves.[32] In this direction different approaches have been proposed so far such as using TiO_2 filler particles with specific shape, surface texture and chemistry for open-channel microfluidics,[33] channels with asymmetry working as diodes,[34] active stooped nanohairs,[35] or pressure driven valving in open paper microfluidics.[36, 37] Again, even though electrowetting and related tools are used widely for this case,[38] cost restrictions and manufacturing complexity is hindering further exploitation, and therefore there is an ongoing demand for novel alternative tools.

We have recently proposed a method for droplet mobility manipulation on flat hydrophobic porous surfaces.[39-42] The significance of pressure difference below and over the liquid phase in droplet adhesion and mobility manipulation has been highlighted, also in other studies.[43-45] Applying a pressure from the rear face of a hydrophobic porous medium (backpressure), the inherently sticky surface is rendered slippery. With deliberate design of the porosity characteristics, sharp transitions between sticky and slippery states may be achieved.

In this work, we present the employment of this general method to manipulate the droplet mobility from flat surfaces, on actuation and valving in fluidics, i.e. confined geometries. Because of the new architecture of the surface, the existence of additional, vertical, walls and the gradual deformation of the liquid from a sessile droplet to a confined plug, the operating conditions and working mechanics differ compared to those on flat surfaces. Open-channel fluidics exhibiting various cross-sections have been prepared to facilitate the backpressure application. The backpressure needed to induce a transition from a sticky to a slippery wall state has been

School of Technological Applications, Technological Educational Institute of Sterea Ellada, Psahna, Greece. Email: nvourdas@teihal.gr; vasta@teihal.gr
Electronic Supplementary Information (ESI) available: Videos and snapshots demonstrating the actuation of one or multiple plugs inside open-channel fluidics. See DOI: 10.1039/x0xx00000x

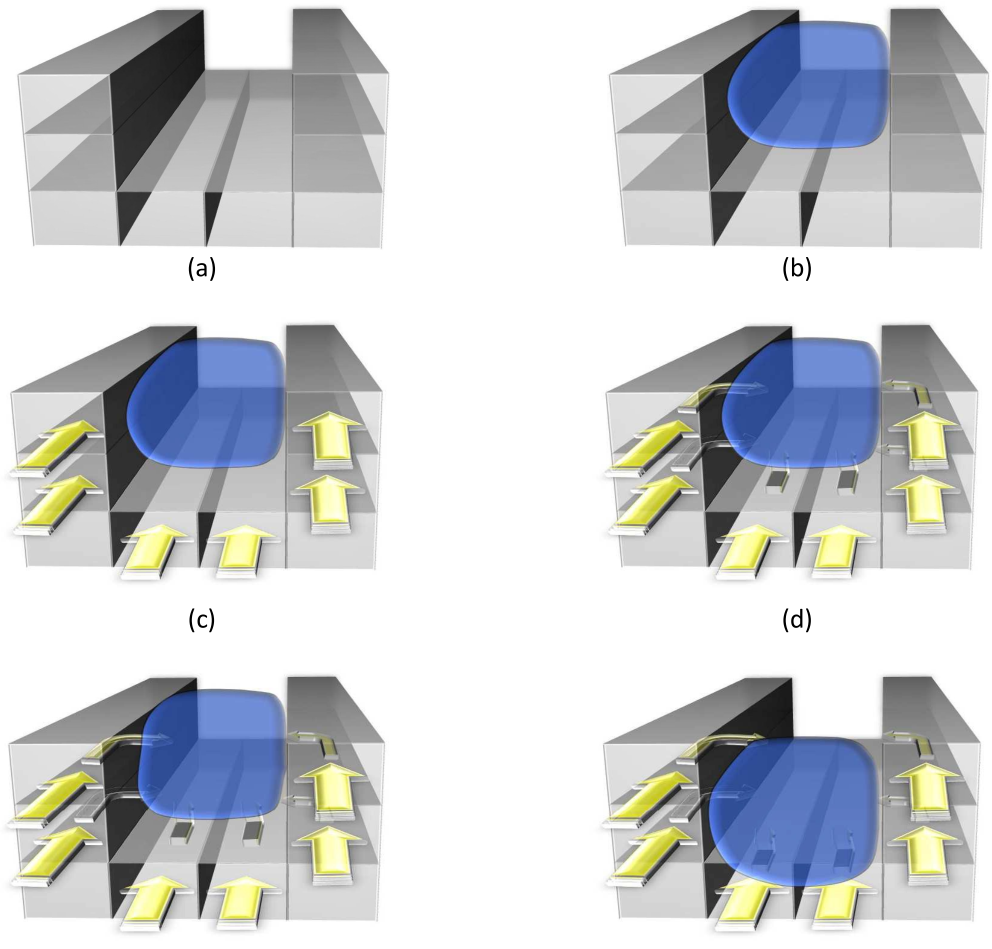

Fig. 1. Schematic representation of the valve architecture and operation. (a) The architecture of the valve. The main channel, of which the walls are porous and hydrophobic, will accommodate the liquid. All other outer walls have been gas sealed. (b) A droplet is introduced in the channel, forming a plug, in this case. (c) Gas flow is applied at the adjacent channels and (d) backpressure increases at the solid-liquid interface. (e) Gas pockets are forming at the interface, (f) rendering the wall slippery and inciting plug flow.

measured for various liquid volumes and tilt angles. The paper is organized as follows: first the basic principle of the tool is described, then we present the experimental results on the minimum backpressure needed to induce the switch from a valve-off to a valve-on state, and finally the mechanics of the plug inside the porous fluidic are briefly analyzed, providing insights on the working principle.

Experimental section

For the fabrication of the open-channel fluidics, commercially available honeycomb-type cellular ceramics of various cells per inch (cpsi) values were used. Such honeycombs are manufactured by mechanical extrusion, drying, de-binding and final sintering ceramics to a typical structure of cordierite ceramics composition ($Al_4Mg_2Si_5O_{18}$), with open unidirectional channels with a square sharing walls. The cordierite honeycomb was cut and machined to the required dimensions and geometry leaving a central channel open on the top face. (Fig. 1). This channel after dry surface modification will serve as the fluidic channel. Use of commercial, low cost, honeycomb structures, instead of laboratory fabricated samples, indicates that such devices exhibit comparative low cost.

These fluidics were treated on a dry vapour deposition reactor, in order to deposit a hydrophobic monolayer. The following procedure was followed. Initially, they were heated to 150 ^oC for 2 h and left to cool down in a desiccator. Then, they were introduced on a vacuum chamber. A solution precursor of 10% 1H,1H,2H,2H-perfluorododecyltrichlorosilane (PFOTS)

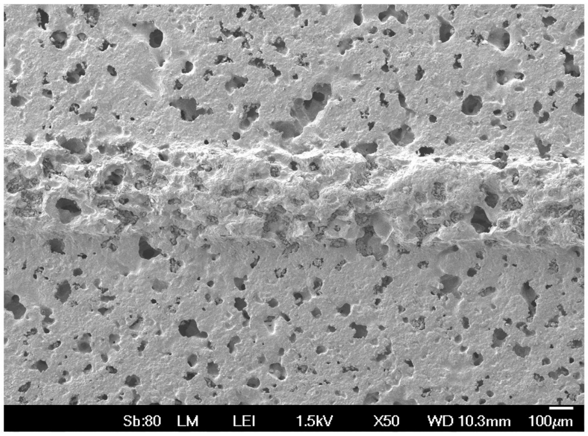

Fig. 2. SEM image of the porous walls of the valve.

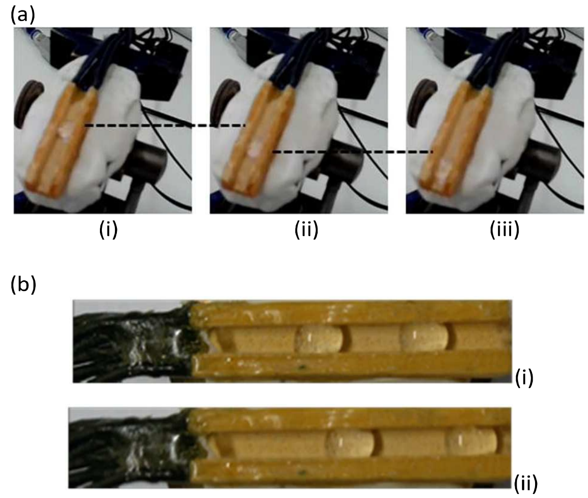

Fig. 3. (a) Snapshots from video showing a droplet moving inside the open-channel fluidic. (i) A droplet has been introduced inside the channel forming a plug, which sticks to the walls. (ii-iii) Plug flows through the channel upon backpressure application. (b) Manipulation of two plugs on the same fluidic simultaneously. The fluidic is tilted downwards on the right side. See ESI.

(purchased from Sigma-Aldrich) in cyclohexane was used, under mild vacuum conditions at 60 ^{o}C. After deposition the surfaces were aged in an oven at 130 ^{o}C for 24 h. After cool down they were used for the experiments. This has been proven adequate for rendering hydrophobic porous structures and 3D internal passages.[46, 47]
Static, receding and advancing water contact angles were measured by a GBX-DIGIDROP at ambient atmospheric conditions. The static water contact angle was ca. 125^{o}. The advancing and receding water contact angles were measured on a water droplet of decreasing/increasing volume. The porous surfaces exhibit receding contact angle ca. 100^{o} and advancing contact angle ca. 135^{o}.
Pressures were measured using the KIMO MP 200HP manometer with 2 mbar accuracy. For every set of parameters no less than five measurements were conducted, and averaged.

Results and discussion

In Fig. 1 we present the basic principle of the active valves developed. For the case depicted in Fig. 1, the valve is rectangular and open from the top face only, however other geometries might be used as well. The central channel, acts as the fluidic channel, while its adjacent channels serve for backpressure application; that is, they allow gas to feed through their porous walls to the fluidic channel.
In Fig. 2 an image of the wall microstructure of the channels is depicted. Both top view and cross section areas show the high porosity of the component. The visible macropores of 10-90 um size are uniformly distributed over a homogeneous and finely sintered cordierite surface. The channel wall is 350-400 um thick, incorporates open and interconnecting macroporosity.
The sintered ceramic walls are highly hydrophilic and water absorbing. Using a dry surface modification, described in the experimental section, a pefluorinated monolayer is deposited, which renders the surfaces hydrophobic, exhibiting a contact angle hysteresis of ca. 35^{o}, indicating a sticky behavior of the surface, and a stationary plug on the fluidic.[48] Detailed, experimentally measured tilt angles, i.e. minimum tilt angle to impart liquid movement are presented later, in this paper.
In Fig. 3a snapshots taken during actuation of a 30 ul plug are illustrated. Initially the plug sticks to the porous surface, because of the hydrophobic character of the walls and the high contact angle hysteresis. With the application of a backpressure, specific values of which are presented below, gas pockets appear at the liquid-solid interface with increasing volume and pressure, which render the walls slippery and triggering the droplet to flow through longitudinally (Fig. 3a(ii-iii)) and downwards due to the gravitational body forces acting on the plug (See electronic supplementary information). The schematic representation of this is illustrated in Fig. 1. This switching is reversible, in that if the backpressure is set off, then the plug will stick again onto the surface; in this case the fluidic acts as a valve and pertinent switching from “off” to “on” may be realized (see video in ESI).
One of the comparable advantages of this tool for actuation and valving is that there are no restrictions related to the point at which the droplet is placed initially on the fluidic channel, since the porous network is not local, but extends all along and across the fluidic. As such, multiple droplets may be manipulated simultaneously. In Fig. 3b we demonstrate the manipulation of two distinct plugs simultaneously on the same fluidic. The fluidic is tilted downwards on the right side. Initially two plugs have been introduced on the fluidic Fig. 3b(i). A backpressure has been applied for a short time period. After

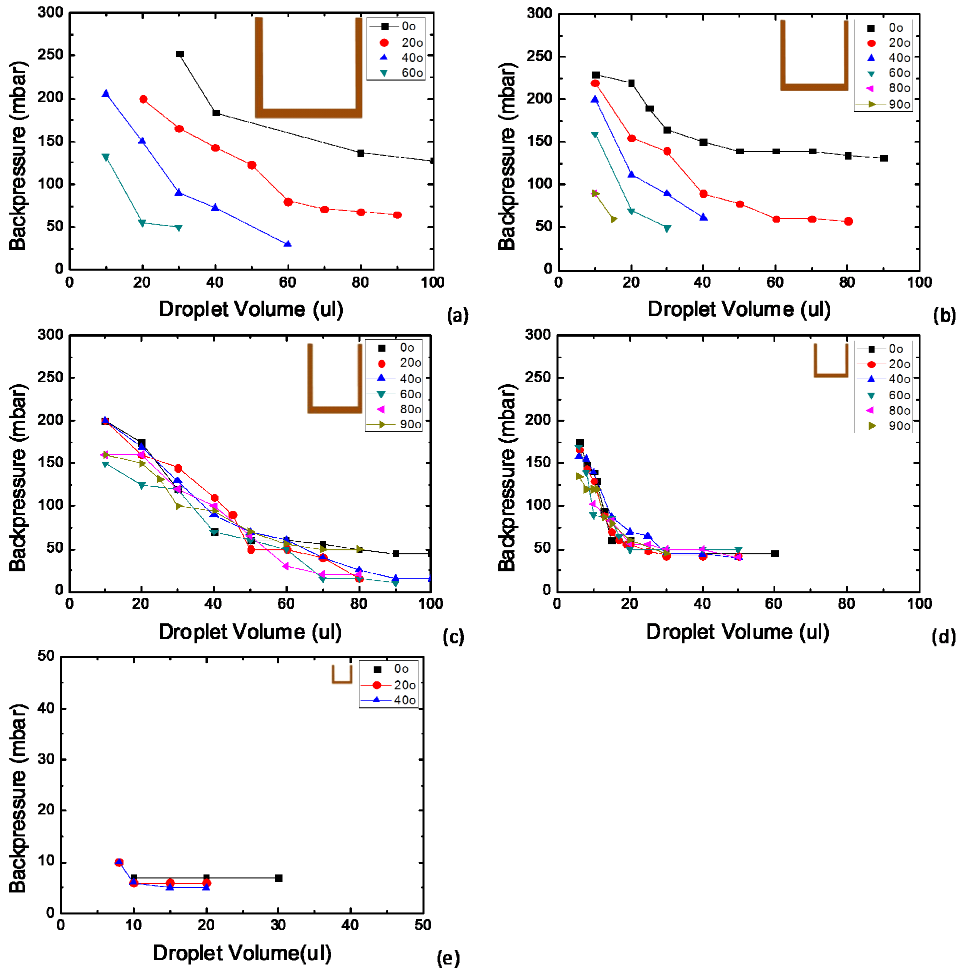

Fig. 4. Experimental measurements of the minimum backpressure for actuation vs. droplet volume and tilt angle for valves with various cross sections: (a) 4.7 mm X 4.7 mm (b) 3.5 mm X 3.3 mm, (c) 3.2 mm X 1.5 mm, (d) 1.5 mm X 1.5 mm, (e) 0.8 mm X 0.8 mm. Insets provide insight of the relative channel dimensions for each case.

the backpressure has been set off the plugs have been moved downwards Fig. 3b(ii) and stick at this point, from which they may be moved only upon re-application of backpressure. When an abrupt increase of backpressure is taking place, the plugs may also be merged (fused) and move along, thus introducing another, additional functionality, i.e. 'droplet merging' (see video in ESI). Moreover fluidics of different geometrical dimensions may facilitate actuation and valving for a wide range of droplet volumes, as described hereafter. Namely, even if a small droplet is introduced inside a wide fluidic without forming a plug, the valve can still manipulate it by adjusting, only the operating parameters.

In Fig. 4a we present the experimental results for the minimum backpressure value needed to actuate a droplet, and hence set the valve-on, on a fluidic of width equal to 4.7 mm and height equal to 4.7 mm. A 10 ul droplet with diameter ~2.7 mm on such fluidic channel may be in touch only at one only of the vertical walls (semi detached). This however imposes no limit to the functionality of the valve; the adequate backpressure is ~210 mbar and ~130 mbar, when tilted at 40^o and 60^o respectively. Further increase of the droplet volume will eventually lead to the formation of plug. The critical plug volume (V_{CR}), i.e. the minimum volume necessary for the water to form the plug in a closed-channel fluidic has been studied versus wettability and geometry in much detail elsewhere and analytical formulas have been extracted.[49] This formula however is not applicable in our case because of the absence of the fourth, namely the top, interface.

For this fluidic after ca. 50 ul the droplet is in contact with both vertical walls, thus forming a plug, the length of which depends on the volume of the droplet. Again the same valve functions, but at different operating parameters. For example in this fluidic (Fig. 4a) and upon 20^{o} tilting, the adequate backpressure decreases gradually from ca. 80 mbar to ca. 70 mbar, when the droplet volume increases from 60 ul to 90 ul.

Lower values of minimum backpressures have been recorded for the fluidic with smaller cross-section, i.e. 3.5 mm width and 3.3 mm height (Fig. 4b). Tilted at 20^{o} the backpressure decreases from ca. 220 mbar to ca. 140 mbar, when the droplet volume increases from 10 ul to 30 ul. After this volume the droplet forms a plug and the minimum backpressure decreases from ca. 90 mbar to ca. 60 mbar when the droplet volume increases from 40 ul to 70 ul and then remains virtually constant. The effect of tilt angle is still profound; for a set droplet volume the minimum backpressure may vary from 20 mbar to 80 mbar for every 20^{o} tilting.

The variation with the tilt angle gradually weakens for fluidics with smaller cross sections. For the case of the fluidic with 3.2 mm width and 1.5 mm height (Fig. 4c), the effect of the tilting angle is less important compared to the previous cases. In this case the backpressure values decrease from ca. 150 mbar to ca. 50 mbar, when the droplet volume increases from 20 ul to 60 ul. The effect of the droplet volume becomes less sensitive after ca. 40 ul droplet volume; while from 20 ul to 40 ul the backpressure decreases 50 mbar, from 50 ul to 70 ul the backpressure decreases only ca. 20 mbar. This plateau evolves at lower droplet volume for the case of the fluidic with 1.5 mm width and 1.5 mm height (Fig. 4d). After ca. 20 ul the backpressures become insensitive not only to the tilting but also to the droplet volume. This implies a significant, and rather interesting versatility for this tool, since no changes at the operating parameters are needed when changing the droplet volume, or if the tilting is changed.

The above mentioned variations depicted on the various fluidics, namely the effect of the tilt angle and the droplet volume on the backpressure, may be justified by calculating the Bond Number (Bo) of the various fluidics:

$$\mathrm{Bo} = \frac{\rho g D^2}{\gamma} \quad \text{Eq.1}$$

with ρ being the liquid density (1000 kg/m^3), g=9.81 m/s^2, D the characteristic length and γ the surface tension (72 mN/m, for water). This dimensionless number correlates the importance of the gravitational body forces compared to the surface tension. Bo scales from 8.72 10^{-2} to 3.07 10^{-1}, to 1.67 and 3.01, when D increases from 0.8 mm, to 1.5 mm, to 3.5 mm and 4.7 mm respectively. As the D increases the importance of the gravitational body forces increase over the surface tension. This is reflected as a gradual increase of the backpressure dependence on the tilt angle and droplet volume. These values however, shall be taken only as indicative, since with the application of backpressure the plug interfaces change drastically; new liquid-gas surfaces evolve and plug geometry gradually transforms.

Of particular interest is the fluidic with cross section of 0.8 mm X 0.8 mm. The fluidic volume in this case is too small and no more that 30 ul may be introduced. This of course depends on the fluidic length. For the experiments conducted and presented in Fig. 4e, the droplet has formed a plug attached to

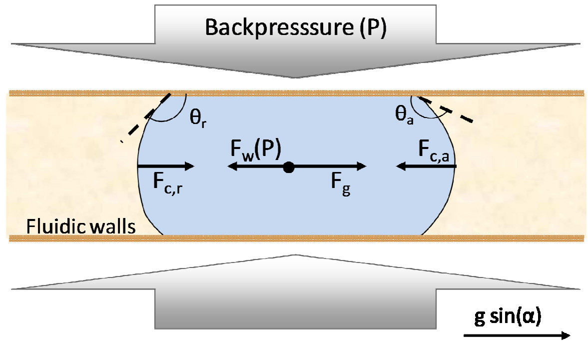

Fig. 5. Forces acting on the plug (simplified scheme).

all three walls. Here, the backpressure is insensitive to both the liquid volume and the tilt angle. Approximately 8 mbar are sufficient to switch the valve on. As such, the operation of the valve becomes rather easy and flexible, in that the valve operates only at two backpressure levels, i.e. 0 and 8 mbar for the "off" and "on" state. It is worth noting, that the very low pressure levels required and, as a consequence, the similarly very low energy demands of the pump as a whole, are compatible with portable, lab-on-chip devices.

In order to gain an insight on the mechanics of the actuation and the mobility manipulation inside the fluidic, and provide an explanation of the operation mechanism, we must account for the forces due to the interfaces and/or the contact lines for a single plug. The case of single droplet/plug on fluidics with various geometries has been studied by using over- or under-pressure along the fluidic,[50-53] spontaneous spreading,[31] or two-phase fluid flow.[54, 55] However, to the best of our knowledge, no analysis has been performed for the actuation scheme utilized in this work, i.e. application of a pressure (backpressure) from the rear side of the hydrophobic porous fluidic walls. In this case gas pockets evolving at the interface introduce newborn gas-liquid interfaces and liquid deformations that are difficult to follow analytically. However we are going to sketch out the main forces implicated in the system.

In general, a single liquid plug within small channel contains two menisci, each with a respective curvature (see Fig. 5). This produces a pressure difference along the phases and the respective force will be denoted as $\mathrm{F_c}$. $\mathrm{F_c}$ is apparent at both the advancing ($\mathrm{F_{c,a}}$) and receding ($\mathrm{F_{c,r}}$) menisci, and prevents the plug to move through the fluidic.[56] $\mathrm{F_c}$ is proportional to the perimeter of the advancing and the receding interface:

$$\mathrm{F_c} = (2\mathrm{h} + \mathrm{w})\, \gamma\, (\cos(\theta_r) - \cos(\theta_a)) \quad \text{Eq.2}$$

where θ_a and θ_r is the advancing and receding contact angle of a droplet on a flat surface (ca. 135^{o} and ca. 100^{o}), w and h are the width and the height of the fluidic.

$\mathrm{F_g}$ is the gravitational body force on the slug:

$$\mathrm{F_g} = \rho\, g\, V \sin s(\alpha) \quad \text{Eq.3}$$

with V being the droplet volume, α being the tilt angle.

Finally, when the plug starts to move, a viscous drag on the liquid by the channel walls, $\mathrm{F_w}$, arises. The exact form of $\mathrm{F_w}$ depends on the the Capillary number ($\mathrm{Ca} = \mu V/\gamma$), namely the plug velocity (V): [55]

$$\mathrm{F_w} = (2\mathrm{h} + \mathrm{w})\,\gamma\,\left[\mathrm{a} + \mathrm{b}\,(\mathrm{Ca})^{2/3}\right] \qquad \text{Eq.4}$$

Upon actuation, $V \to 0$ and hence $\mathrm{Ca} \to 0$. a is a parameter that depends on the geometrical characteristics of the fluidic and scales with $(\cos(\theta_r) - \cos(\theta_a))$. A typical value for a on a solid hydrophobic rectangular channel is a=0.5.[53] In our case, the drag of the plug depends also on the backpressure applied (P), i.e. $F_w = F_w(P)$. In general as the backpressure increases F_w also decreases.

Let us assume the case of a 20 ul droplet plug on the 0.8 mm X 0.8 mm fluidic, tilted at α=40^{o} (Fig. 4e). The aforementioned forces become: $\mathrm{F_c}$= 9.22 10^{-5} N, $\mathrm{F_g}$=1.26 10^{-4} N. Using the tabulated value for a=0.5 yields to $\mathrm{F_w}$=8.64 10^{-4} N. Even though initially $\mathrm{F_c}$<$\mathrm{F_g}$, the plug does not move because $\mathrm{F_g}$<$\mathrm{F_w}$. In order for the plug to move a backpressure value of P=8 mbar is needed, which lowers the $\mathrm{F_w}$ marginally below 1.26 10^{-4} N.

This simple approach simplifies the physical system, mainly by ignoring the effect of the deformations induced by the gas pockets evolving at the interfaces, as well as the effects of the respective Laplace pressures introduced in the system. These effects are also asymmetric due to buoyancy forces exerted on the gas pockets, and therefore cannot be easily followed analytically. In any case both the $\mathrm{F_c}$ and the $\mathrm{F_w}$ change dramatically upon backpressure application.

Conclusions

We presented a tool for actuation and valving in microfluidics, utilizing the manipulation scheme for liquid droplet/plug mobility on hydrophobic porous surfaces, by means of backpressure. With this, the gas pockets characteristics at the liquid-solid interface are controlled, which in turn play a crucial role at the mechanics of the plug adhesion. Fluidics of different cross sections have been fabricated and characterized. Initially, the fluidic surfaces are sticky, pugs are pinned and hence the valve is off. Applying backpressure the surfaces gradually become slippery, plugs are actuated and flow through, thus switching the valve to the on position. The adequate backpressure for various cross sections and water volumes has been measured. As the cross section becomes smaller the effect of the volume and the tilt angle gradually weakens. For the fluidic of 0.8 mm x 0.8 mm size, the backpressure value is only ca. 8 mbar, and the effect of tilt angle and droplet volume can be ignored. This value is very low and is directly related to the ultra low energy demands of the entire device. With this tool the use of electromagnetic energy, foreign particles, oily phases, or moving elements is avoided. The liquid phase remains unaffected both chemically and thermally. The proposed tool for actuation and valving is also amenable to integration in miniaturized, low power, portable devices such as microfluidics, and lab-on-chip devices, as well as in large scale applications. Conclusions from this study may apply also to the management of water plugs in proton exchange membrane (PEM) fuel cells.

Acknowledgements

John S. Latsis Public Benefit Foundation is kindly acknowledged for financial support through the “Research Projects 2015” Grant.

References

1. P. G. de Gennes, F. Brochard-Wyart and D. Quere, *Capillarity and Wetting Phenomena: Drops, Bubbles, Pearls, Waves*, Spinger-Verlag, New York, 2004.
2. C.-H. H. Choi, U. Ulmanella, J. Kim, C. M. Ho and C. J. Kim, *Physics of Fluids*, 2006, **18**, 087105.
3. E. Gogolides, K. Ellinas and A. Tserepi, *Microelectronic Engineering*, 2015, **132**, 135-155.
4. M. Kitsara and J. Ducrée, *Journal of Micromechanics and Microengineering*, 2013, **23**, 033001.
5. E. Gogolides, M. Vlachopoulou, K. Tsougeni, N. Vourdas and A. Tserepi, *International Journal of Nanomanufacturing*, 2010, **6**, 152-163.
6. N. Vourdas, A. Tserepi, A. Boudouvis and E. Gogolides, *Microelectronic Engineering*, 2008, **85**, 1124-1127.
7. N. T. Nguyen, presented at the 3rd European Conference on Microfluidics-Microfluidics 2012, Heidelberg, December 3-5, 2012, 2012.
8. R. Seemann, M. Brinkmann, T. Pfohl and S. Herminghaus, *Reports on progress in physics*, 2012, **75**, 016601.
9. S.-Y. Teh, R. Lin, L.-H. Hung and A. P. Lee, *Lab on a chip*, 2008, **8**, 198-220.
10. J. V. I. Timonen, M. Latikka, L. Leibler, R. H. A. Ras and O. Ikkala, *Science*, 2013, **341**, 253-257.
11. T. Verho, J. T. Korhonen, L. Sainiemi, V. Jokinen, C. Bower, K. Franze, S. Franssila, P. Andrew, O. Ikkala and R. H. A. Ras, *Proceedings of the National Academy of Sciences*, 2012, **109**, 10210–10213.
12. G. Pashos, G. Kokkoris and A. G. Boudouvis, *Langmuir*, 2015, **31**, 3059-3068.
13. S. Wang, T. Wang, P. Ge, P. Xue, S. Ye, H. Chen, Z. Li, J. Zhang and B. Yang, *Langmuir*, 2015, **31**, 4032-4039.
14. T. Wang, H. Chen, K. Liu, Y. Li, P. Xue, Y. Yu, S. Wang, J. Zhang, E. Kumacheva and B. Yang, *Nanoscale*, 2014, **6**, 3846-3853.
15. Y. Feng, Z. Zhou, X. Ye and J. Xiong, *Sensors and Actuators A: Physical*, 2003, **108**, 138-143.
16. K. Tsougeni, D. Papageorgiou, A. Tserepi and E. Gogolides, *Lab on a Chip - Miniaturisation for Chemistry and Biology*, 2010, **10**, 462-469.
17. K. Ellinas, A. Tserepi and E. Gogolides, *Microfluid Nanofluid*, 2014, **7**, 1-10.
18. K. Hosokawa and R. Maeda, *Journal of micromechanics and microengineering*, 2000, **10**, 415.

19. Q. Yu, J. M. Bauer, J. S. Moore and D. J. Beebe, *Applied Physics Letters*, 2001, **78**, 2589-2591.
20. V. Studer, G. Hang, A. Pandolfi, M. Ortiz, W. F. Anderson and S. R. Quake, *Journal of Applied Physics*, 2004, **95**, 393-398.
21. D. B. Weibel, M. Kruithof, S. Potenta, S. K. Sia, A. Lee and G. M. Whitesides, *Analytical chemistry*, 2005, **77**, 4726-4733.
22. J.-H. Choi, S.-K. Lee, J.-M. Lim, S.-M. Yang and G.-R. Yi, *Lab on a chip*, 2010, **10**, 456-461.
23. J. W. Choi, S. Lee, D. H. Lee, J. Kim, A. J. Demello and S. I. Chang, *RSC Advances*, 2014, **4**, 20341-20345.
24. D. Moschou, N. Vourdas, G. Kokkoris, G. Papadakis, J. Parthenios, S. Chatzandroulis and A. Tserepi, *Sensors and Actuators B: Chemical*, 2014, **199**, 470-478.
25. S. K. Cho, H. Moon and C.-J. Kim, *Microelectromechanical Systems, Journal of*, 2003, **12**, 70-80.
26. F. Mugele and J.-C. Baret, *Journal of Physics: Condensed Matter*, 2005, **17**, R705.
27. M. G. Pollack, A. D. Shenderov and R. B. Fair, *Lab on a chip*, 2002, **2**, 96-101.
28. B. J. Toley, J. A. Wang, M. Gupta, J. R. Buser, L. K. Lafleur, B. R. Lutz, E. Fu and P. Yager, *Lab on a Chip - Miniaturisation for Chemistry and Biology*, 2015, **15**, 1432-1444.
29. K. Choi, A. H. C. Ng, R. Fobel and A. R. Wheeler, *Annual review of analytical chemistry*, 2012, **5**, 413-440.
30. M. Abdelgawad and A. R. Wheeler, *Advanced Materials*, 2009, **21**, 920-925.
31. B. P. Casavant, E. Berthier, A. B. Theberge, J. Berthier, S. I. Montanez-Sauri, L. L. Bischel, K. Brakke, C. J. Hedman, W. Bushman, N. P. Keller and D. J. Beebe, *Proceedings of the National Academy of Sciences of the United States of America*, 2013, **110**, 10111-10116.
32. Y. Temiz, R. D. Lovchik, G. V. Kaigala and E. Delamarche, *Microelectronic Engineering*, 2015, **132**, 156-175.
33. A. Ghosh, R. Ganguly, T. M. Schutzius and C. M. Megaridis, *Lab on a chip*, 2014, **14**, 1538-1550.
34. J. Feng and J. P. Rothstein, *Journal of Colloid and Interface Science*, 2013, **404**, 169-178.
35. T.-i. Kim and K. Y. Suh, *Soft Matter*, 2009, **5**, 4131-4135.
36. A. C. Glavan, R. V. Martinez, E. J. Maxwell, A. B. Subramaniam, R. M. Nunes, S. Soh and G. M. Whitesides, *Lab on a chip*, 2013, **13**, 2922-2930.
37. A. C. Glavan, R. V. Martinez, A. B. Subramaniam, H. J. Yoon, R. M. D. Nunes, H. Lange, M. M. Thuo and G. M. Whitesides, *Advanced Functional Materials*, 2014, **24**, 60-70.
38. M. Abdelgawad, S. L. S. Freire, H. Yang and A. R. Wheeler, *Lab on a chip*, 2008, **8**, 672-677.
39. N. Vourdas, C. Ranos and V. N. Stathopoulos, *RSC Advances*, 2015, **5**, 33666-33673.
40. N. Vourdas and V. N. Stathopoulos, presented at the Technical Proceedings of the 2014 NSTI Nanotechnology Conference and Expo, NSTI-Nanotech 2014, 2014.
41. N. Vourdas, A. Tserepi and V. N. Stathopoulos, *Applied Physics Letters*, 2013, **103**, 111602.
42. V. N. Stathopoulos and N. Vourdas, presented at the The 8th International Conference on Material Technologies and Modeling, MMT 2014, 2014, 2014.
43. T. M. Schutzius, S. Jung, T. Maitra, G. Graeber, M. Köhme and D. Poulikakos, *Nature*, 2015, **527**, 82-85.
44. J. Snoeijer, P. Brunet and J. Eggers, *Physical Review E*, 2009, **79**, 036307.
45. J. de Ruiter, R. Lagraauw, D. van den Ende and F. Mugele, *Nat Phys*, 2014, **11**, 48-53.
46. N. E. Vourdas, M. E. Vlachopoulou, A. Tserepi and E. Gogolides, *International Journal of Nanotechnology*, 2009, **6**, 196-207.
47. A. Milionis, C. Noyes, E. Loth, I. S. Bayer, A. W. Lichtenberger, V. N. Stathopoulos and N. Vourdas, *Materials and Manufacturing Processes*, 2015, in press.
48. R. Finn, *Equilibrium capillary surfaces*, Springer Science & Business Media, 2012.
49. A. Herescu and J. S. Allen, *Journal of Power Sources*, 2012, **216**, 337-344.
50. K. Hosokawa, T. Fujii and I. Endo, *Analytical chemistry*, 1999, **71**, 4781-4785.
51. K. Handique, D. T. Burke, C. H. Mastrangelo and M. A. Burns, *Analytical Chemistry*, 2001, **73**, 1831-1838.
52. H. A. Stone, A. D. Stroock and A. Ajdari, *Annu. Rev. Fluid Mech.*, 2004, **36**, 381-411.
53. M. J. Cheah, I. G. Kevrekidis and J. B. Benziger, *Langmuir*, 2013, **29**, 9918-9934.
54. C. N. Baroud, F. Gallaire and R. Dangla, *Lab on a chip*, 2010, **10**, 2032-2045.
55. C. P. Ody, *Microfluid Nanofluid*, 2010, **9**, 397-410.
56. T. S. Sammarco and M. A. Burns, *AIChE Journal*, 1999, **45**, 350-366.